

Yeast Rrp14p is required for ribosomal subunit synthesis and for correct positioning of the mitotic spindle during mitosis

Marlene Oeffinger³, Alessandro Fatica^{1,2}, Michael P. Rout³ and David Tollervey^{1,*}

¹Wellcome Trust Centre for Cell Biology, University of Edinburgh, Edinburgh EH9 3JR, Scotland, UK, ²Department of Genetics and Molecular Biology, University of Rome 'La Sapienza', P. Aldo Moro, 5, 00185 Rome, Italy and

³Rockefeller University, 1230 York Avenue, New York, NY10021, USA

Received September 11, 2006; Revised and Accepted October 5, 2006

ABSTRACT

Here we report that Rrp14p/Ykl082p is associated with pre-60S particles and to a lesser extent with earlier 90S pre-ribosomes. Depletion of Rrp14p inhibited pre-rRNA synthesis on both the 40S and 60S synthesis pathways. Synthesis of the 20S precursor to the 18S rRNA was largely blocked, as was maturation of the 27SB pre-rRNA to the 5.8S and 25S rRNAs. Unexpectedly, Rrp14p-depleted cells also showed apparently specific cell-cycle defects. Following release from synchronization in S phase, Rrp14p-depleted cells uniformly arrested in metaphase with short mitotic spindles that were frequently incorrectly aligned with the site of bud formation. In the absence of Bub2p, which is required for the spindle orientation checkpoint, this metaphase arrest was not seen in Rrp14p-depleted cells, which then arrested with multiple buds, several SPBs and binucleate mother cells. These data suggest that Rrp14p may play some role in cell polarity and/or spindle positioning, in addition to its function in ribosome synthesis.

INTRODUCTION

The majority of steps in ribosome synthesis take place within the nucleolus, a specialized subnuclear structure. In the budding yeast *Saccharomyces cerevisiae*, the nucleolus is formed around the highly repetitive rDNA array on chromosome XII. Here, the rDNA is transcribed into a large precursor RNA (pre-rRNA), which is subsequently modified and then matured by endonuclease and exonuclease processing to yield the mature 18S, 5.8S and 25S rRNAs (see Figure 1). Ribosome synthesis is a major activity in the Eukaryotic cell and a rapidly growing yeast cell produces around

2000 ribosomes per minute. Both the size of the cell at division and number of ribosomes per cell, are closely linked to growth rate [reviewed in (1,2)]. Moreover, both size at division and ribosome numbers anticipate the future growth rate suggesting a cross-talk mechanism between ribosome synthesis and mitotic cell division (3). Recent studies in yeast have identified several connections among the nucleolus, ribosome biogenesis and cell-cycle progression [reviewed in (4)]. A small number of ribosomal processing factors were found that appear to facilitate cross-talk between those processes, with mutations in these proteins affecting both ribosome synthesis and cell division (5–10).

Ykl082c/Rrp14p is an essential protein that was initially characterized in two-hybrid analyses of a protein interaction network involved in the specification of cell polarity (11). Rrp14p interacted with Bud8p, a component of the distal bud site tag complex, Zds2p, a nucleolar protein with a role in cell polarity as well as gene silencing (12,13), and with Gic1p and Gic2p, which interact directly with the GTPase Cdc42, a key regulator of cell polarity (14–16). Strains carrying *gic1/2Δ* have a depolarized actin and microtubule cytoskeleton, implicating these proteins in microtubule polarization and nuclear migration. Rrp14p was therefore proposed to be involved in polarized growth and the establishment of bud sites, although direct physical interactions were not assessed (11).

YFP-tagged Rrp14p was found to localize to the nucleolus (11), and we subsequently identified Rrp14p as a component of an early pre-60S complex that was co-purified with tagged Ssf1p (17), suggesting a role in ribosome synthesis. Rrp14p is a member of the SURF-6 family of nucleolar proteins, which have been predicted from bioinformatic analyses to participate in complex protein–protein and protein–RNA interactions within the nucleolus (18–20).

Here we report that Rrp14p functions in ribosome synthesis; it is required for the maturation of both small and large subunit rRNAs and helps to prevent premature cleavage of the pre-rRNA at site C₂. Strains depleted of Rrp14p also

*To whom correspondence should be addressed. Tel: +44 131 650 7092; Fax: +44 131 650 7040; Email: d.tollervey@ed.ac.uk

Present address:

Marlene Oeffinger, Rockefeller University, 1230 York Avenue, New York, NY10021, USA

© 2007 The Author(s).

This is an Open Access article distributed under the terms of the Creative Commons Attribution Non-Commercial License (<http://creativecommons.org/licenses/by-nc/2.0/uk/>) which permits unrestricted non-commercial use, distribution, and reproduction in any medium, provided the original work is properly cited.

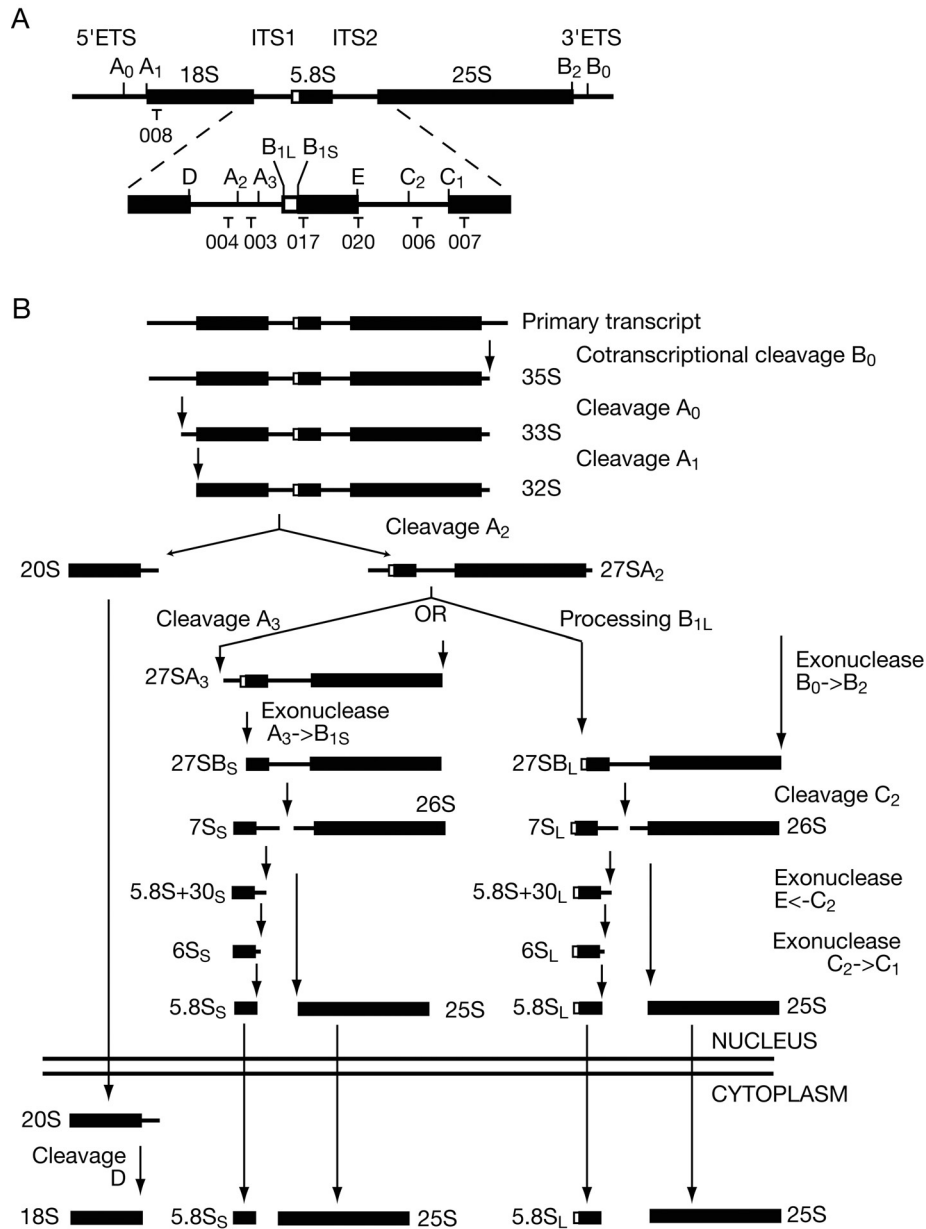


Figure 1. Yeast pre-rRNA and processing. (A) Structure of the yeast pre-rRNA, with locations of oligonucleotides used as hybridization probes. (B) Pre-rRNA processing pathway showing the intermediates detected by pulse-chase and northern analyses.

show defects in positioning and elongation of the mitotic spindle during mitosis, which were not previously reported for cells depleted for any other ribosome synthesis factor.

MATERIALS AND METHODS

Strains and molecular techniques

Standard techniques were employed for growth and handling of yeast. Yeast strains used in this work are listed in Supplementary Table S1. Strain YAF32 was created from BMA38 by use of a one-step PCR strategy as described previously (21). TAP-tagging of Rrp14p was performed as described in (22). Strain YMO22 was created by integration of a Cdc14-GFP-Trp1 construct (kindly provided by

E. Schiebel). Strains YMO111, YMO102 and YMO104 were created from KH230 (kindly provided by K. Hardwick) and YMO103 and YMO105 from W303, respectively, by one-step PCR strategy (21) and homologous recombination of the linearized plasmid PRE10.1, carrying a MAD2::URA3 deletion cassette. YMO200 and YMO201 were created by crossing with YFC2160-16C. YMO202 was created by crossing with VAY371.

Oligonucleotides

For RNA hybridizations, the following oligonucleotides were used: 001, 5'-CCAGTTACGAAAATTCTTG; 002, 5'-GCTC-TTTGCTCTTGCC; 003, 5'-TGTTACCTCTGGGCC; 004, CGGTTTTAATTGTCCTA; 005, 5'-ATGAAAACCTCCACA-

GTG; 006, 5'-GGCCAGCAATTTCAAGTTA; 007, 5'-CTC-CGCTTATTGATATGC; 008, 5'-CATGGCTTAATCTTTG-AGAC; 017, 5'-GCGTTGTTTCATCGATGC; 020, 5'-TGAG-AAGGAAATGACGCT; 033, 5'-CGCTGCTCACCAATGG; and 041, 5'-CTACTCGGTCAGGCTC.

RNA extraction, northern hybridization and primer extension

For depletion of the Rrp14p protein, cells were harvested at intervals following a shift from RGS medium (2% raffinose, 2% galactose and 2% sucrose), or YPGal medium (2% galactose), to YPD medium (2% glucose). Otherwise strains were grown in YPD medium except for over-expression studies for which strains were grown in RGS medium. RNA was extracted as described previously (23). Northern hybridizations and primer extension analysis were carried out as described in (23). Standard 1.2 or 2% agarose/formaldehyde and 6% acrylamide/urea gels were used to analyze the high and low molecular weight RNA species, respectively.

Sucrose gradient analysis and affinity purification

Sucrose gradient centrifugation was performed as described previously (24,25). RNA was extracted from each fraction and resolved on standard 1.2% agarose/formaldehyde gels. Mature rRNAs and pre-rRNA species were detected by ethidium staining and northern hybridization, respectively. Sedimentation of proteins was assayed by SDS-PAGE and TAP-tagged Rrp14p was detected by western immunoblotting with peroxidase-conjugated rabbit IgG (SIGMA). Affinity purification of TAP-tagged Rrp14 and analysis of co-purified RNAs was performed as described previously (17).

Pulse-chase labeling

Metabolic labeling of RNA was performed as described previously (17). The strains *GAL::HA-rrp14* and BMA38 were transformed with a plasmid containing the *URA3* gene, pre-grown in galactose medium lacking uracil and transferred to glucose minimal medium for 6 h. Cells at 0.3 OD_{600nm} were labeled with [5,6-³H]uracil for 1 min

followed by a chase with excess unlabeled uracil. Standard 1.2% agarose/formaldehyde and 6% polyacrylamide/urea gels were used to analyze the high and low molecular weight RNA species, respectively.

Immunofluorescence

GAL::HA-rrp14, *GAL::HA-rrp14/CDC14-GFP*, *GAL::HA-rrp14/mad2Δ*, *mad2Δ*, *GAL::HA-rrp14/bub2Δ*, *bub2Δ* and wild-type strains with and without Spc42-GFP were pre-grown in RGS medium, containing 2% raffinose, 2% galactose and 2% sucrose, and harvested at intervals following a shift to medium containing 2% glucose. For arrest in early S phase, cells were pre-synchronized by a 2 h treatment with alpha-factor (10 μM), performed 2 h after shift to glucose containing medium (26). Cells were then transferred to pre-warmed glucose medium lacking alpha-factor but containing 0.1 M hydroxyurea for a further 2 h. Cells were released from arrest into pre-warmed glucose medium. Samples, taken after 0, 20, 40 and 60 min, were fixed by incubation in 4% (v/v) formaldehyde at 25°C for 3 min for SPB visualization, or 1 h for tubulin, Cdc14-GFP and Nop1p detection, and then spheroplasted. Immunofluorescence was performed as described previously (27,28). Tubulin was detected with a rabbit anti-tubulin antibody (Sigma) and a secondary goat anti-rabbit antibody coupled to FITC (Sigma) at 1:1000 and 1:200 dilutions, respectively. Nop1p was detected with mouse anti-Nop1p (29) and a secondary goat anti-mouse antibody coupled to FITC (Sigma). Cover slips were mounted using moviol, containing DAPI. The cells were examined under a Zeiss Axioscop fluorescent microscope. Pictures were obtained with Smart Capture VP and Openlab.

FACS analysis

To determine DNA content, cells were harvested 0, 20, 40 and 60 min after release from early S phase arrest, and fixed for 1 h in 70% ethanol at RT. Cells were washed twice in 50 mM Tris (pH 7.5) and resuspended in 1 mg/ml RNase A in 50 mM Tris, pH 7.5. RNase A digestion was performed for 4 h at 37°C. Cells were then washed and

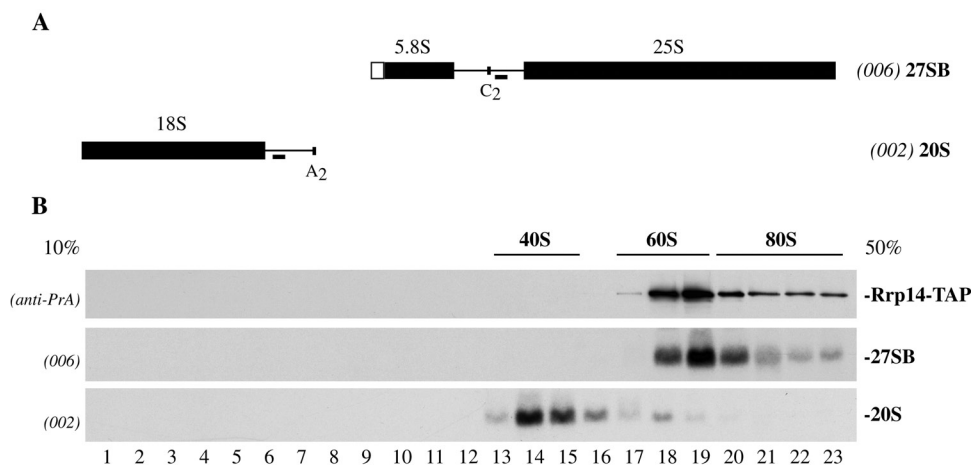


Figure 2. Rrp14p cosediments with pre-60S ribosomes. (A) Pre-rRNA species detected and locations of oligonucleotide probes. (B) Lysate from a strain expressing an Rrp14p-TAP fusion was fractionated on a 10–50% sucrose gradient. Fractions were analyzed by western blotting for the distribution of Rrp14p-TAP and by northern hybridization for the distribution of the 27SA and 27SB pre-rRNA components of the pre-60S ribosome and the 20S component of pre-40S.

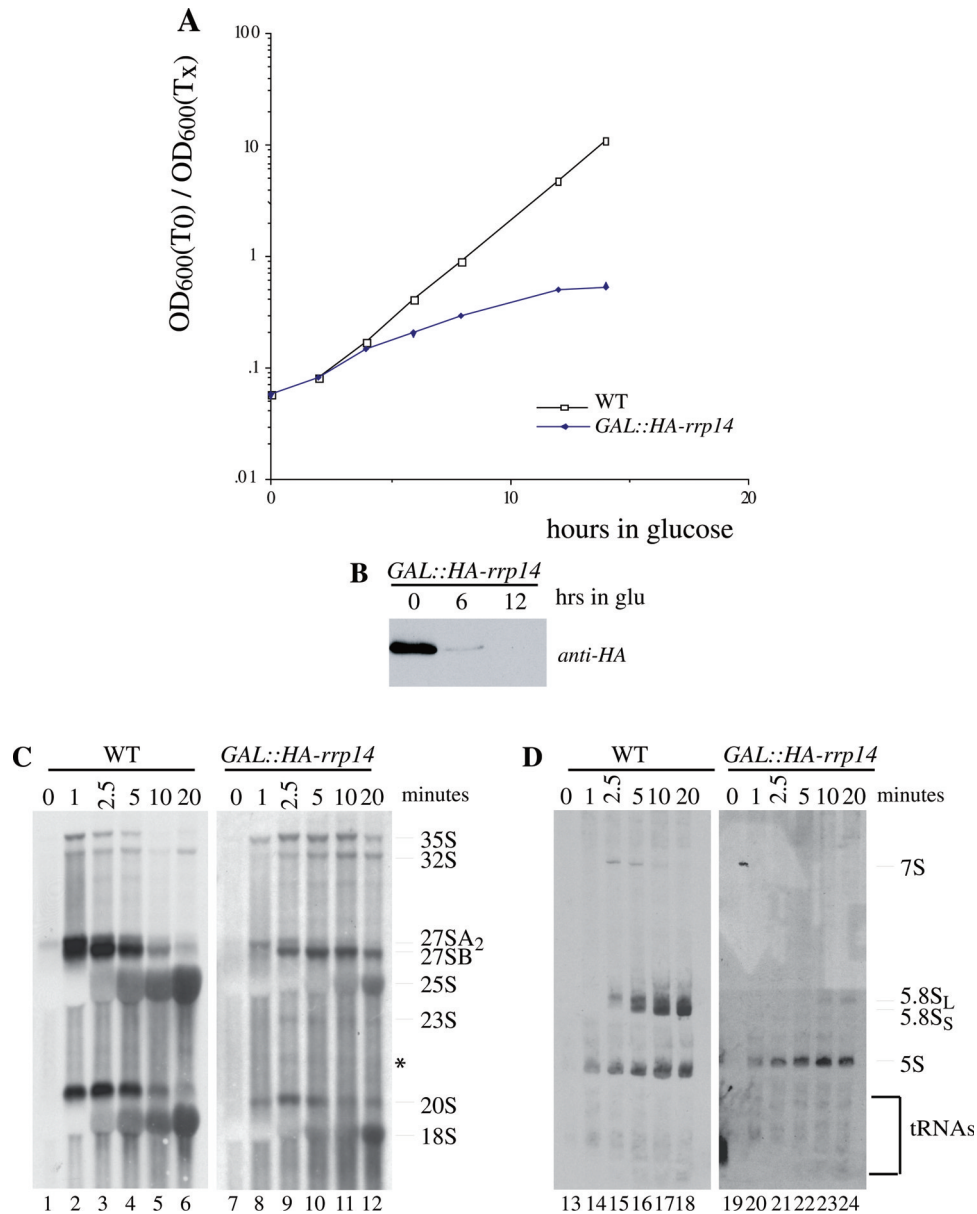


Figure 3. Depletion of Rrp14p impairs growth and 60S subunit synthesis. (A) Growth of *GAL::HA-rrp14* (crosses) and otherwise isogenic wild-type (open boxes) strains following transfer to glucose medium. (B) Western analysis of the depletion of HA-Rrp14p on glucose medium. (C and D) Pulse-chase labeling of rRNA synthesis in *GAL::HA-rrp14* wild-type strains 7 h after transfer to glucose medium. Cells were pulsed with [5,6-³H]uracil for 1 min and then chased with a large excess of unlabeled uracil for the times indicated. (C) High molecular weight RNA analyzed on a 1.2% agarose/formaldehyde gel. (D) Low molecular weight RNA analyzed on a 6% polyacrylamide/urea gel. RNA species are labeled on the right of the panels. The asterisk in (C) indicates the position of the putative 5'ETS-D species.

resuspended in 40 µg/ml Proteinase K, and incubated for 1 h at 55°C. The cells were harvested and resuspended in 50 µg/ml propidium iodine in PBS, pH 7.2, and then sonicated at low power for 5 s to separate loosely associated cells. Determination of DNA content was performed on a Becton-Dickinson FACScan.

RESULTS

Rrp14p associates with pre-60S particles

Rrp14p (Ykl082c) was identified by mass spectrometry in precipitates of TAP-tagged ribosome synthesis factors Ssf1p

and Rrp1p, both of which are components of early pre-60S ribosomal particles (17,30,31), suggesting that Rrp14p is also a component of early pre-60S ribosomes. To determine whether Rrp14p is associated with pre-ribosomal particles, we constructed a strain expressing a C-terminal fusion between a TAP tag (22) and Rrp14p. The fusion construct was inserted into the genome under the control of the *RRP14* promoter and supported wild-type growth, showing it to be functional (data not shown). To assess the association of Rrp14p with pre-ribosomal particles, a sucrose gradient analysis was performed with a lysate from the Rrp14-TAP strain. The sedimentation of Rrp14-TAP was determined by western blotting with antibodies that recognize the protein

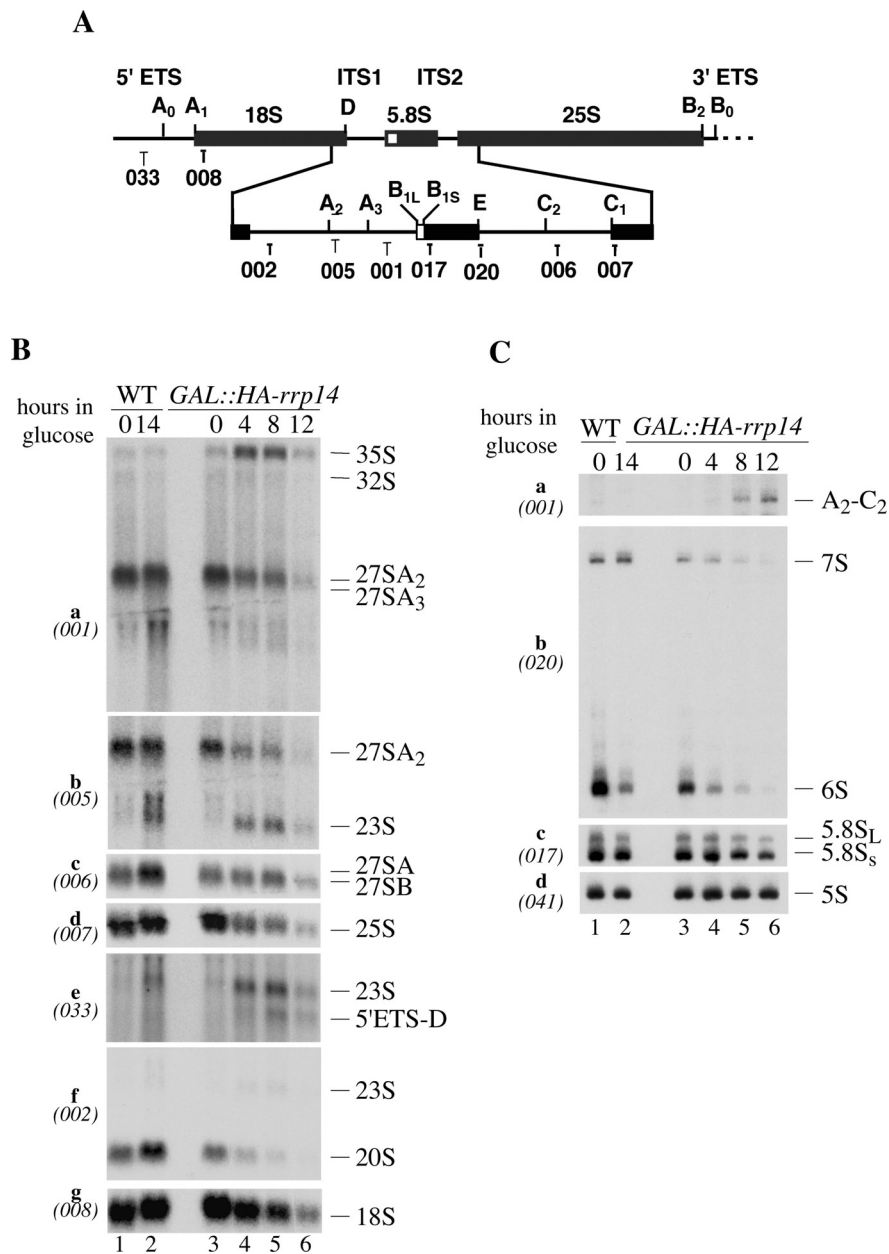


Figure 4. Rrp14p is required for pre-rRNA processing. (A) Schematic diagram of the pre-rRNA showing the processing sites and locations of oligonucleotide probes used. (B) Northern analyses of high molecular weight RNA separated on a 1.2% agarose/formaldehyde gel. (C) Northern analyses of low molecular weight RNA separated on a 6% polyacrylamide/urea gel. RNA species are labeled on the right of the northern panels. Oligonucleotide probes used are on the right.

A moiety of the TAP tag, and compared with the rRNA species and pre-rRNAs (Figure 2). Comparison with the positions of the mature rRNAs detected by ethidium staining (data not shown and indicated by bars on Figure 2B) and the pre-rRNAs indicated that Rrp14-TAP is most enriched in the 60S region of the gradient, with a weaker peak ~80–90S. No cosedimentation with the 20S pre-rRNA was observed, indicating that Rrp14p is not associated with 40S pre-ribosomes. These analyses are consistent with the previous proteomic data indicating that Rrp14p is present in pre-60S particles, but additionally suggest an association with 90S pre-ribosomes, within which the early assembly of the 40S subunit occurs.

Rrp14p is required for rRNA synthesis

To determine the requirement for Rrp14p in rRNA synthesis, we integrated an N-terminal HA-Rrp14p fusion construct under the control of the repressible *GAL1* promoter at the endogenous *RRP14* locus (21) (see Materials and Methods). The *GAL::HA-rrp14* strain grew more slowly than the isogenic wild type in galactose media, indicating that Rrp14p over-expression is toxic. However, growth of the *GAL::HA-rrp14* strains was identical to the wild type in RGS medium (containing raffinose, sucrose and galactose), which results in lower expression levels, and shortly after transfer to glucose medium (Figure 3A), showing the HA-fusion construct to be functional. Growth of the *GAL::HA-rrp14* strain was strongly

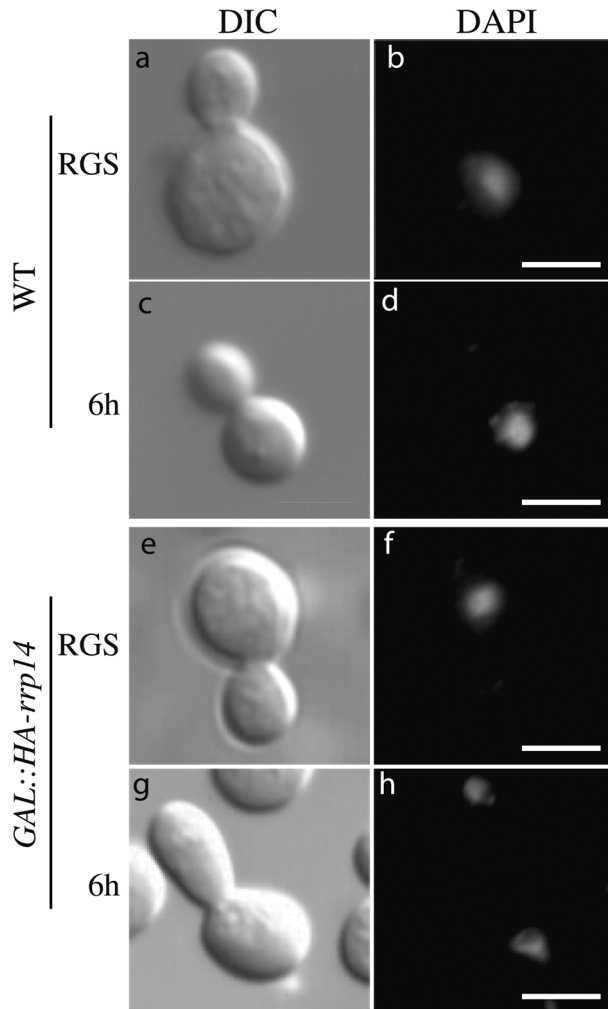


Figure 5. Rrp14p depleted cells arrest with a distinctive morphology. Cells were pre-grown in RGS medium and depleted of Rrp14p by growth of *GAL::HA-rrp14* in glucose medium for 6 h. The nucleoplasm was visualized by staining of the DNA with DAPI. Cell morphology was visualized by differential interference contrast (DIC) microscopy.

reduced 6 h after transfer to glucose media and had almost ceased by 12 h. Consistent with this, western blotting (Figure 3B) showed that HA-Rrp14p was strongly depleted after 6 h in glucose and undetectable after 12 h.

Pre-rRNA processing was initially assessed by pulse-chase labeling *in vivo* with [5,6-³H]uracil 7 h after transfer to glucose medium. Analysis of high molecular weight RNA (Figure 3C) showed that in the Rrp14p-depleted strain 35S and 32S pre-rRNAs accumulated, whereas the 27SA pre-rRNA was less abundant and its conversion to 27SB and mature 25S rRNA was greatly reduced. The level of 20S pre-rRNA was reduced with the concomitant appearance of the aberrant 23S molecule and synthesis of mature 18S was both delayed and reduced. The 23S RNA originates from direct cleavage of the 35S pre-rRNA at site A₃ when the cleavages at sites A₀, A₁ and A₂ are delayed.

The formation of low molecular weight rRNAs (5S and 5.8S) was analyzed by PAGE (Figure 3D). In the Rrp14p-depleted strain, the 7S pre-rRNA was not readily detected

and very low levels of the mature 5.8S rRNA accumulated (Figure 3D). The mature 5.8S_L and 5.8S_S are the products of alternative processing pathways. No change in their ratio was seen, indicating that Rrp14p is required for 27SB pre-rRNA processing in both pathways.

To further characterize pre-rRNA processing in the *GAL::HA-rrp14* mutant strain, steady-state levels of mature and precursor rRNA molecules were assessed by northern hybridization of RNAs resolved on agarose gels (Figure 4B) or polyacrylamide gels (Figure 4C). Rrp14p-depletion led to strong accumulation of the 35S pre-rRNA and appearance of the 23S RNA, whereas levels of the 27SA₂ and 20S pre-rRNAs were reduced (Figure 4B), consistent with inhibition of cleavage at sites A₀, A₁ and A₂. An aberrant RNA, which is predicted to extend from the end of the 5' ETS to site D, was also accumulated (5'ETS-D in Figure 4B) and a band of appropriate mobility was seen in the pulse-chase labeling (marked with asterisk in Figure 3C). This species is presumably generated by pre-rRNA processing in ITS1 and 3' maturation of 18S rRNA, in the absence of processing in the 5'ETS. On the pathway of 60S synthesis, the 27SB pre-rRNA was not strongly reduced at the 4 and 8 h depletion time points, whereas the mature 25S was depleted, showing that its maturation was prevented. Analyses of low molecular weight RNAs (Figure 4C) showed that levels of the later 7S and 6S pre-rRNAs were reduced, with a more rapid effect on 6S. In addition, an aberrant species that extend from A₂ to C₂ was accumulated (Figure 4C, panel a), which results from premature cleavage of the 27SA₂ pre-rRNA at site C₂. The appearance of the A₂-C₂ fragment was described previously in strains lacking Ssf1p and Ssf2p (17) and other pre-60S components (4,32,33).

We conclude that Rrp14 is required for pre-rRNA maturation on both the 40S and 60S pathways.

Rrp14p depletion arrests cell-cycle progression

Rrp14p was reported to interact with proteins required for cell polarity (11). We, therefore, inspected cells undergoing Rrp14p depletion by microscopy, to determine whether they arrest at a specific stage of the cell cycle. Following transfer to glucose medium for 6 h, 62% of *GAL::HA-rrp14* cells (from 650 cells examined) showed a distinctive and unusual morphology (Figure 5, panel g). The cells were arrested with large buds, which were generally more elongated than those seen in the wild-type (Figure 5, panels a-d) or in *GAL::HA-rrp14* cells growing in permissive, RGS medium (Figure 5, panel e). Cell-cycle arrest with large, elongated buds was previously reported for cells defective in the mitotic exit network (MEN) (34,35) or depleted of the ribosome synthesis factor Nop15p, which causes an arrest at cytokinesis (6). However, in each of these cases the cells arrest with separated nuclei whereas Rrp14p-depleted cells arrest with a single nucleus, as shown by DAPI staining of the DNA (Figure 5, panel h). These observations suggested that, in addition to its role in ribosome synthesis, Rrp14p is required at a specific step in cell-cycle progression, after commitment to bud formation but before nuclear division.

To better analyze this defect, wild-type and *GAL::rrp14* cells were synchronized in early S phase using alpha-factor, followed by hydroxyurea (HU) arrest and release.

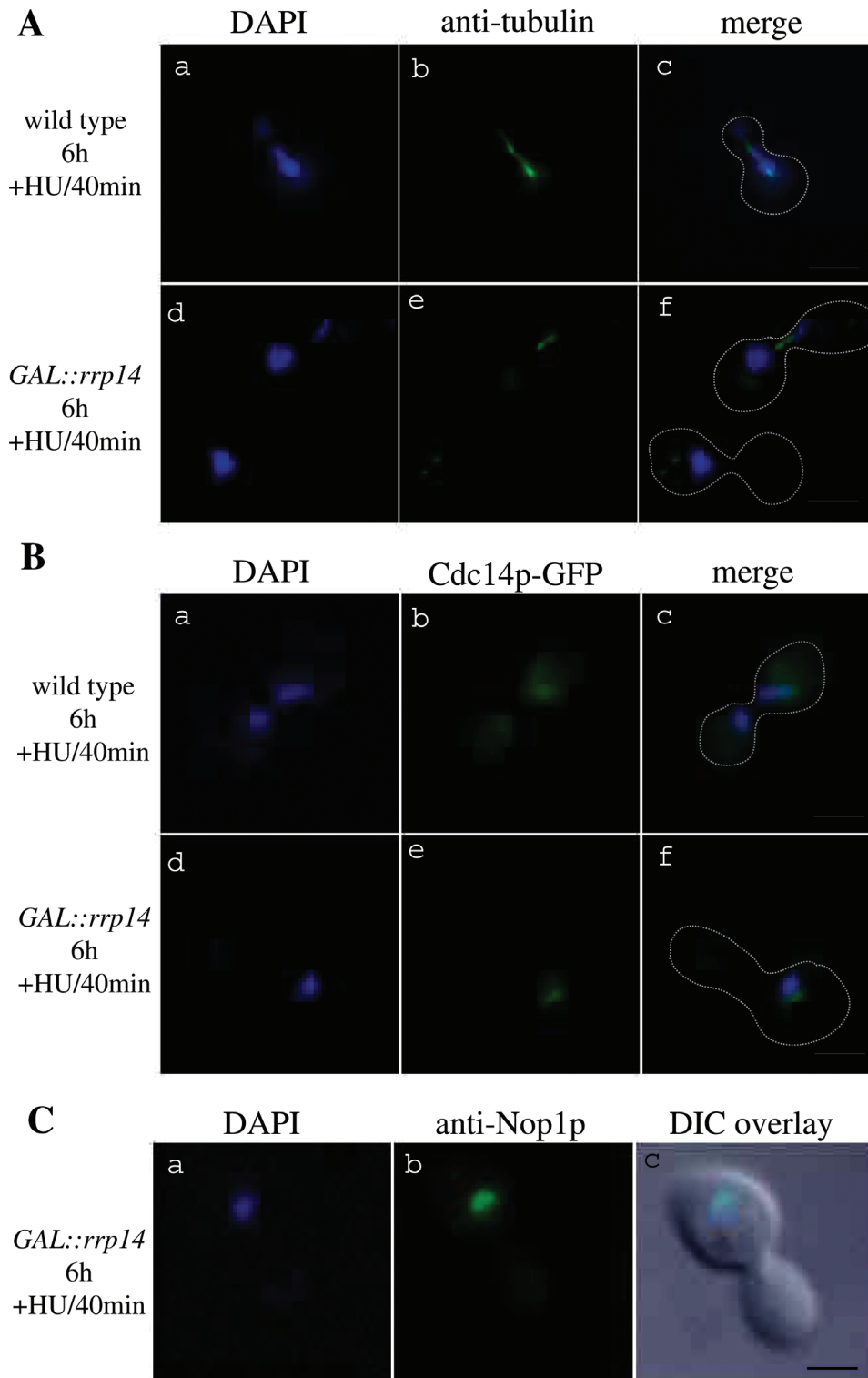








Figure 6. Spindle orientation and elongation are impaired in synchronized, Rrp14p-depleted cells. Wild type, *GAL::HA-rrp14* and *GAL::HA-rrp14/CDC14-GFP* cells were shifted to glucose medium for 2 h and then treated with alpha-factor for 2 h, arresting the cells at the G₁/S phase boundary. Cells were transferred to glucose medium lacking alpha-factor but containing hydroxyurea (HU) for a further 2 h, arresting cells in early S phase. Cells were fixed and analyzed 40 min after release from HU arrest. (A) Rrp14p-depleted cells contain short mitotic spindles that are often miss positioned and lack cytoplasmic microtubules (panels d–f). DNA was visualized by DAPI staining (panels a and d). Tubulin was visualized by staining with rabbit anti-tubulin antibody and goat anti-rabbit coupled to FITC (panels b and e). Cell outlines are indicated with a dotted line (panels c and f). (B) Cdc14p–GFP remains associated with the nucleolus in cells arrested by Rrp14p depletion (panel e). Cell outlines are indicated with a dotted line (panels c and f). (C) Localization of the nucleolus following depletion of Rrp14p. The nucleolar marker Nop1p was visualized with mouse anti-Nop1p antibody and goat anti-rabbit coupled to FITC (panel b). Bars represent 10 μm.

Table 1. Cell morphology in wild-type and Rrp14-depleted cells

Strain	% (n = 650)	
		
(a) Nuclear separation and spindle location in WT and Rrp14-depleted cells		
Wild-type	100	0
<i>GAL::rrp14</i>	3	97
		
	68	29
Strain	% (n = 400)	
		
(b) Cdc14p-release in WT and Rrp14-depleted cells		
Wild-type	89	11
<i>GAL::rrp14</i>	0	100

Wild-type, *GAL::HA-rrp14* and *GAL::HA-rrp14/CDC14-GFP* cells were shifted to glucose medium for 2 h and then treated with alpha-factor for 2 h, arresting the cells at the G₁/S phase boundary. Cells were transferred to glucose medium lacking alpha-factor but containing hydroxyurea (HU) for a further 2 h, arresting cells in early S phase. Cells were fixed and analyzed 40 min after release from HU arrest.





a: Nuclei were visualized by DAPI staining, formation and elongation of the mitotic spindle was examined by staining with a rabbit anti-tubulin antibody. Ninety-seven percent of Rrp14p-depleted from 650 examined cells were arrested before nuclear separation during the first round of cell division. Out of these, 68% contained spindles that was within or adjacent to the bud-neck with either correct or perpendicular orientation; 29% of cells had spindles that did not lie close to the budneck and were apparently randomly positioned in the mother cell cytoplasm.

b: In 89% of wild-type cells (from 400 examined), Cdc14p-GFP is released from the nucleolus into the nucleoplasm. Cdc14p-GFP remains associated with the nucleolus in 100% of Rrp14p-depleted cells.

Commencing 2 h after transfer to glucose medium, cells were initially pre-synchronized at the G₁ to S phase boundary by alpha-factor treatment for 2 h, and then released from the alpha-factor block into HU for 2 h. Following HU release, wild-type cells proceeded rapidly through nuclear separation and cell division, as reported previously (26). In contrast, 97% of Rrp14p-depleted cells (from 650 cells examined) were arrested before nuclear separation during the first round of cell division. Formation and elongation of the mitotic spindle was examined by staining with a rabbit anti-tubulin antibody (Figure 6A, panels b and e; quantified in Table 1a). In Rrp14p-depleted cells, the spindle poles were duplicated and clearly separated, but were closely positioned, indicating arrest during elongation of the mitotic spindle. In 68% of arrested cells the spindle was within or adjacent to the bud neck with either correct or perpendicular orientation. Strikingly, however, 29% of Rrp14p-depleted cells had spindles that did not lie close to the bud-neck and were apparently randomly positioned in the mother cell cytoplasm (Figure 6A and Table 1a). Furthermore, cytoplasmic microtubules (MTs) were not visible.

In wild-type cells the spindle pole body (SPB) is normally localized adjacent to the site of the developing bud, and this is an important determinant of cell polarity (36,37).

Table 2. Spindle pole body localization and spindle orientation in wild-type and Rrp14-depleted cells.

Strain	% (n = 650)			
				
Wild-type	100	0	0	0
<i>GAL::rrp14</i>	4	62	34	0
Wild-type/ <i>mad2Δ</i>	100	0	0	0
<i>GAL::rrp14/mad2Δ</i>	5	65	30	0
Wild type/ <i>bub2Δ</i>	100	0	0	0
<i>GAL::rrp14/bub2Δ</i>	4	8	22	66

Cells were treated as described in Table 1. SPB localization, visualized using Spc42-GFP, and spindle orientation visualized by staining with rabbit anti-tubulin antibody and goat anti-rabbit coupled to FITC, were analyzed. Percentages derived from 650 cells examined. Although the SPB localization and spindle orientation were normal in wild-type, *bub2Δ* and *mad2Δ* single deletion strains, it was strongly affected in *GAL::HA-rrp14* and *GAL::HA-rrp14/mad2Δ* *GAL::HA-rrp14/bub2Δ* cells upon depletion of Rrp14p.

The mislocalization of the SPB in cells lacking Rrp14p would be consistent with a function in cell polarity (11).

In wild-type cells undergoing mitosis, Cdc14p is released from the nucleolus into the nucleoplasm (38–40). To follow its location, a Cdc14p-GFP fusion (35) (kindly provided by E. Schiebel) was expressed in the wild-type and *GAL::HA-rrp14* strains. As shown in Figure 6B and Table 1b, by 40 min after HU release Cdc14p-GFP had delocalized from the nucleolus to the nucleoplasm in 89% of wild-type cells (from 400 examined) but remained restricted to the nucleolus in all Rrp14p-depleted cells.

Since Rrp14p is normally nucleolar, we checked the location and integrity of the nucleolus in the Rrp14p-depleted cells by immunofluorescence with antibodies against the nucleolar marker Nop1p. Anti-Nop1p decorated a crescent-shaped region slightly displaced from the DAPI-stained nucleoplasm, in a pattern characteristic of the normal yeast nucleolus (Figure 6C). The nucleolus and nucleoplasm both remained undivided in the Rrp14p-depleted cells following HU release. In wild-type cells, the nucleolus is predominantly localized opposite the SPB during interphase (41), but moves to a position perpendicular to the mitotic spindle before division. In 76% of Rrp14p-depleted cells (from 600 cells examined) this reorganization did not occur, as shown by the position of the Nop1p signal opposite the bud site (Figure 6C, panel c).

To confirm the conclusions on the defects in the localization of the mitotic spindle, the *GAL::HA-rrp14* mutation was combined with a construct expressing a fusion between the SPB protein Spc42p and green fluorescent protein (GFP) (Figure 7; quantified in Table 2). In the wild-type strain 40 min after HU release (Figure 7, panels a–d), the nucleus and SPBs had been segregated and migrated into the bud. In contrast, in the Rrp14p-depleted cells (Figure 7, panels e–h) the SPBs had not segregated and were not correctly aligned with the bud site.

Defects in either the structure of the mitotic spindle or in the attachment of chromosomes to the spindle are sensed by checkpoint systems, leading to cell-cycle arrest at metaphase with short spindles, as seen in Rrp14p-depleted cells [reviewed in (42)]. There are two distinct spindle checkpoint

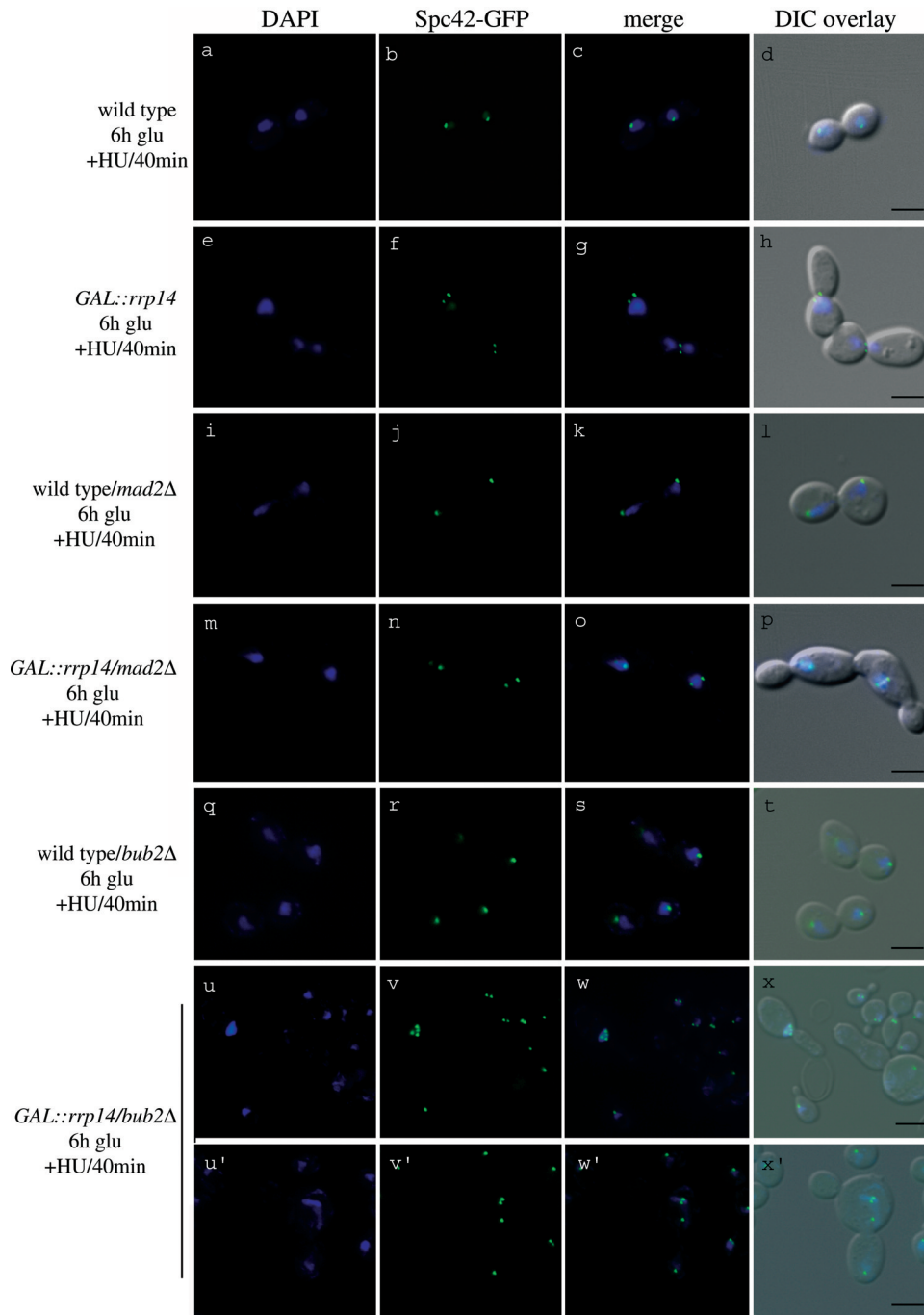


Figure 7. The Bub2p spindle orientation check-point is responsible for cell-cycle arrest following Rrp14p depletion. Cells were treated as in Figure 6. SPB localization was visualized using Spc42-GFP, in wild type (panel b), *GAL::HA-rrp14* (panel f), *mad2Δ* (panel j), *GAL::HA-rrp14/mad2Δ* (panel n), *bub2Δ* (panel r) and *GAL::HA-rrp14/mad2Δ* (panels v and v') cells 40 min after HU release. Nuclei were visualized by DAPI staining (panels a, e, i, m, q, u and u'). Cell morphology was observed by DIC (panels d, h, l, p, t, x and x'). Bars represent 10 μ m.

pathways in yeast responding to separable MT-dependent events; the Mad2p pathway or spindle assembly checkpoint, and the Bub2p or spindle orientation checkpoint (43,44). To assess whether either of these pathways was responsible for the observed cell-cycle arrest, *GAL::HA-rrp14* was combined with the *mad2Δ* and *bub2Δ* deletions. The *mad2Δ* single mutation had little effect on spindle formation in the *RRP14*⁺ strain (Figures 7, panels i–l, and 8, panels a–c, and

Table 2). When Rrp14p was depleted from the *mad2Δ* cells (Figures 7, panels m–p, and 8, panels d–f) the phenotype closely resembled the depletion of Rrp14p alone (Figure 7, panels e–h) with no increase in spindle elongation or the frequency of nuclear division, and a similar fraction of cells contained a spindle and nucleus that were not located near the bud neck (30% of 650 cells counted) (Figure 7, panels m–p, and Table 2).

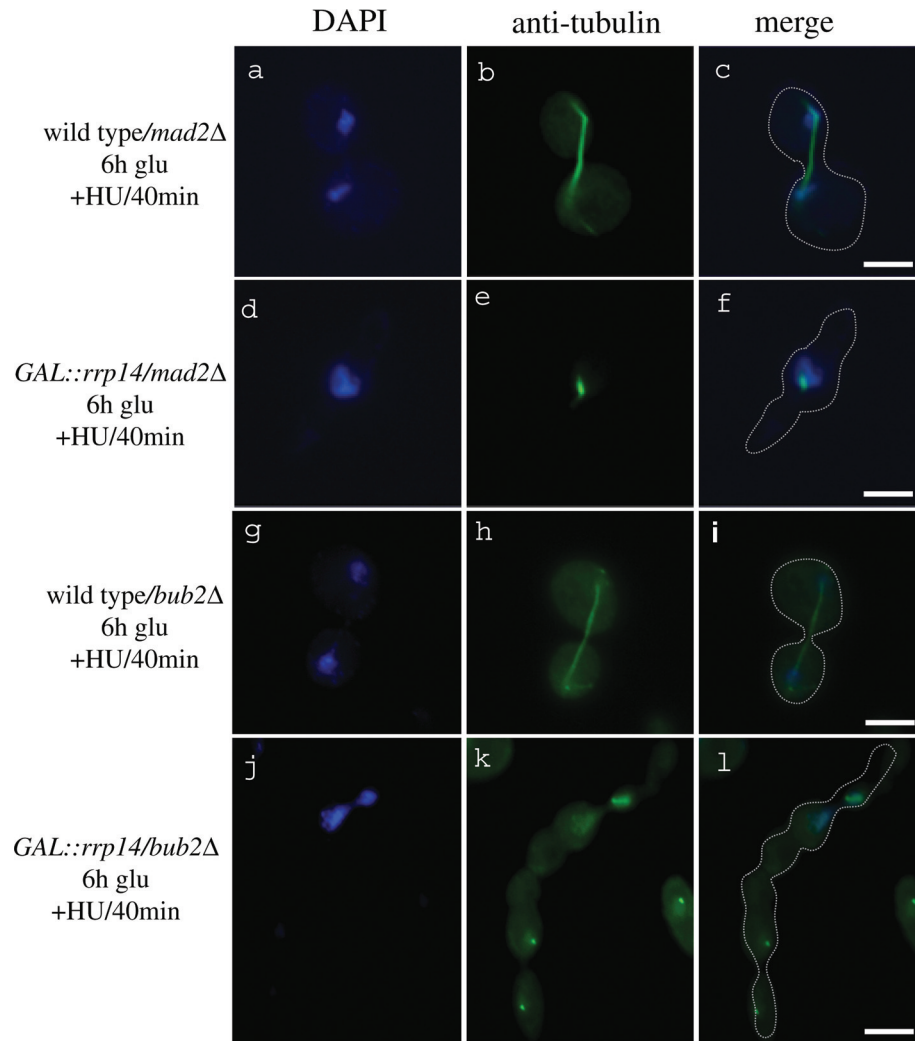


Figure 8. Cells form multiple spindles following Rrp14p depletion in *bub2Δ* spindle checkpoint mutants. Cells were treated as in Figure 6. Tubulin was visualized by staining with rabbit anti-tubulin antibody and goat anti-rabbit coupled to FITC, in *mad2Δ* (panel b), *GAL::HA-rrp14/mad2Δ* (panel e), *bub2Δ* (panel h) and *GAL::HA-rrp14/mad2Δ* (panel k) cells 40 min after HU release. Nuclei were visualized by DAPI staining (panels a, d, g and j). Cell outlines are indicated with a dotted line (panels c, f, i and l).

The *bub2Δ* single mutant also showed no effect on spindle formation (Figures 7, panels q–t, and 8, panels g–i, and Table 2), but clearly exacerbated the phenotype when Rrp14p was depleted. Ninety-six percent of cells (from 650 cells counted) displayed abnormal spindle orientation with the majority of cells (66%) also containing multiple SPBs, deformed nuclei or binucleate mother cells (Figures 7, panels u–x, and 8, panels j–l, and Table 2). Many cells apparently continued to bud despite the defect in cell division, forming chains of cells (Figures 7, panels x, x', and 8, panel l). We conclude that activation of the Bub2p spindle checkpoint is responsible for the cell-cycle arrest in cells depleted of Rrp14p.

Recent reports have implicated other 60S ribosome synthesis factors in the mechanism of DNA replication (5,45,46). A failure to undergo DNA replication following HU release would potentially explain some, but not all, of the defects observed in Rrp14p-depleted cells. DNA replication was followed by fluorescence-activated cell sorting (FACS) analysis at intervals following release from HU arrest

(Figure 9). In unsynchronized cells (Figure 9A) the two major peaks correspond to cells with unreplicated (1C) and duplicated (2C) genomes. In both the wild type and mutant, the HU-induced block was efficient with most cells arrested with a 1C genome (Figure 9B and C). In the wild type, most cells had undergone DNA replication 20 min after HU release, and almost all after 40 min (Figure 9B). By 60 min after HU release, haploid cells that have completed mitosis were reappearing. In the Rrp14p-depleted cells, DNA replication is slower, with more cells remaining 1C or in S phase at 20 and 40 min after release than in the wild type (Figure 9C). However, at 40 min after HU release, the time at which the microscopy presented in Figures 6, 7 and 8 was performed, most cells appear to have completed DNA replication, indicating that this is unlikely to be the major cause of the cell-cycle arrest in Rrp14p-depleted cells. In the *GAL::HA-rrp14* strain the absence of Mad2p or Bub2p had no clear effects on DNA replication, nor did loss of the genome integrity check point protein Mec1p (47) (data not shown).

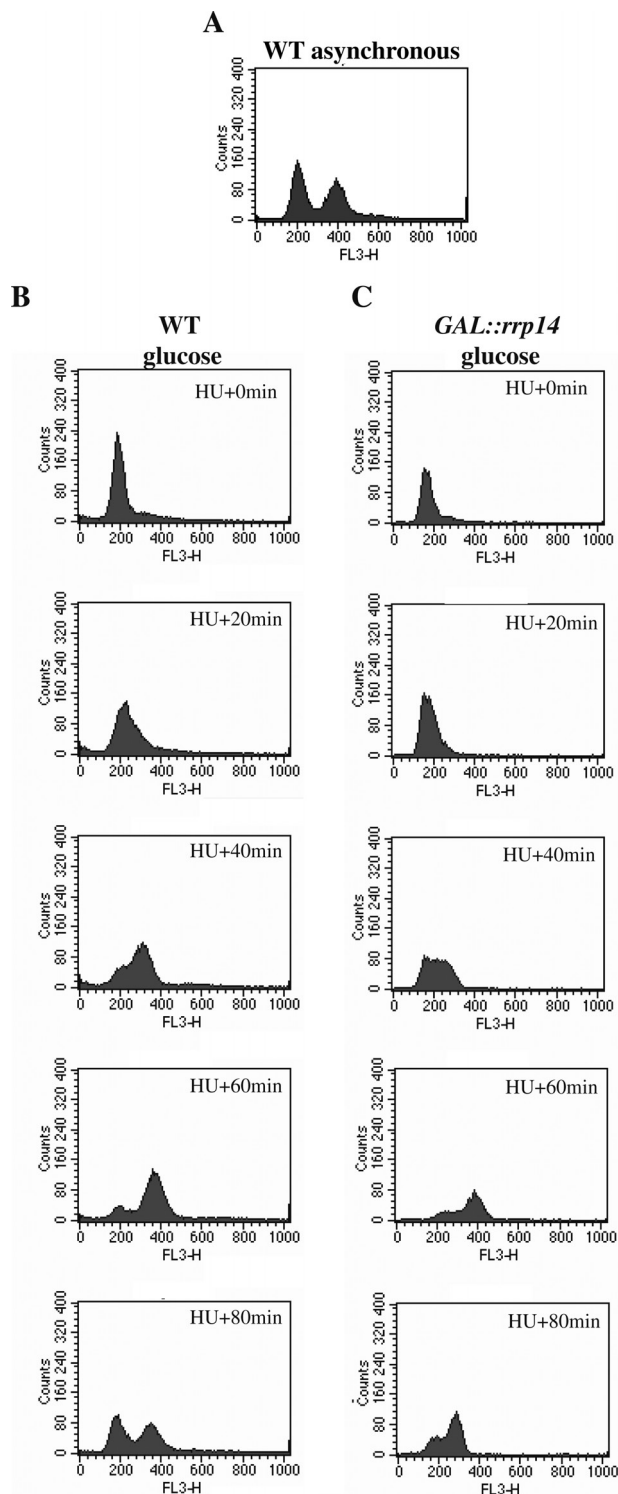


Figure 9. DNA replication is only mildly slowed in Rrp14p-depleted cells but nuclei do not separate. (A) FACS analysis of unsynchronized wild-type cells. The left-hand peak represents the 1N cell population, while the right-hand peak corresponds to 2N cells that have undergone DNA replication. FACS analyses of wild-type (B) and *GAL::HA-rrp14* cells (C), synchronized in early S phase by alpha-factor and HU treatment in glucose medium, as described for Figure 5. Following HU release, cells were fixed and analyzed after 0, 20, 40, 60 and 80 min, as indicated. It is likely that a fraction of the Rrp14p-depleted cells are arrested at the Start checkpoint before DNA replication initiation, due to reduced ribosome synthesis. These probably correspond to the cells that remain haploid after release from HU.

DISCUSSION

Here we report that yeast Rrp14p functions in the synthesis of both 40S and 60S ribosomal subunits and may also play some direct role in cell-cycle progression through G_2/M . Rrp14p was identified as a putative participant in 60S ribosomal subunit synthesis by its co-precipitation with early pre-60S particles that were associated with TAP-tagged Ssf1p (17) and Rrp1p (30). However, gradient analyses indicate that Rrp14p also associates with the earlier 90S pre-ribosomes, which include many of the factors required for 40S ribosome synthesis. In addition to inhibiting rRNA maturation, loss of Rrp14p apparently allowed premature cleavage of both the 35S and 27SA₂ pre-rRNAs. We speculate that Rrp14p binds late pre-90S particles and then remains associated with the pre-60S region. As well as promoting correct maturation of both subunits, Rrp14p might act to suppress ITS1 and ITS2 cleavage until other maturation steps have occurred.

In addition to their unusual pre-rRNA processing defects, cells depleted of Rrp14p showed striking cell-cycle-related phenotypes. It is difficult to exclude the possibility that these are an indirect consequence of reduced ribosomal subunit abundances. However, this seems unlikely because no similar phenotypes have been reported for any of the large number of ribosome synthesis factors previously analyzed. This phenotype is certainly not expected to result from the inhibition of translation *per se*, which leads to cell-cycle arrest at the 'Start' check point at the G_1-S boundary and this is also seen in many strains with ribosome synthesis defects [(46,48) and reviewed in (49)]. Rrp14p was initially characterized in two hybrid analyses of a protein interaction network involved in the specification of cell polarity, and was predicted to be involved in polarized growth and the establishment of bud sites (11). Although these authors did not demonstrate the physical association of Rrp14p with proteins direct involved in cell polarity, their conclusions are at least consistent with our observations.

Synchronized Rrp14p-depleted cells arrest with an undivided nucleus and short spindles, a phenotype characteristic of arrest at the G_2/M boundary. Moreover, the spindles are often misaligned with the bud axis, and the nuclei frequently fail to migrate to the bud neck. In wild-type cells the nucleolus moves during mitosis from its S phase location opposite the bud neck to a position perpendicular to the bud neck (50). In most Rrp14p-depleted cells the nucleolus was incorrectly positioned, remaining located opposite the bud neck. The cytoplasmic MT asters, which normally form on the cytoplasmic face of the SPBs, were also absent in Rrp14p-depleted cells.

In several mutant strains cell-cycle arrest during mitosis has been shown to be a consequence of activation of checkpoints, which respond to defects in DNA replication, spindle structure or spindle orientation. A mild delay in DNA replication was seen in Rrp14p-depleted cells, but this was very much less marked than the inhibition seen in cells depleted of another 60S synthesis factor, Yph1p, which associates with the DNA origin of replication complex (ORC) (5,51). Moreover, 40 min after release from HU arrest, most Rrp14p-depleted cells have completed DNA replication, as judged by FACS analysis, but all are arrested at G_2/M as

judged by their morphology. It is therefore unlikely that a failure in DNA replication is responsible for the cell-cycle arrest.

Defects in the structure of the mitotic spindle or its attachment to chromosomal centromeres are monitored by the Mad2p-dependent spindle checkpoint, while defects in spindle orientation activate a Bub2p-dependent checkpoint (52,53) [reviewed in (42)]. To determine whether either of these checkpoints arrests Rrp14p-depleted cells, we deleted the genes encoding Mad2p and Bub2p. The absence of Mad2p had no clear effects on the growth, DNA replication or morphology of Rrp14p-depleted cells. In contrast, the absence of Bub2p from Rrp14p-depleted cells led to the formation of cells containing multiple SPBs, binucleate mother cells and cell chains, presumably due to ongoing bud formation and SPB duplication without cell division. This observation indicates that the defect in the orientation of the spindles in Rrp14p-depleted cells is responsible for the cell-cycle arrest.

RNAs have been identified in the centrioles of surf clams (54), whereas RNA species associate with mitotic MTs in *Xenopus* egg extracts and spindle assembly is promoted by the RNA export factor Rae1p (55), which is structurally related to the spindle checkpoint protein Bub3p (56). Yeast Rae1p (Gle2p) (57) is implicated in the export of ribosomal subunits (58,59), but potential interactions with Rrp14p have not been directly assessed. Furthermore, a proteomic analysis of 60S pre-ribosomal particles isolated from human cells identified MT-associated proteins as components of the complex (60).

Together these data suggest that in other systems RNA molecules associate with mitotic spindles, and it is at least conceivable that RNAs—and therefore RNA-binding proteins—also play some role in yeast spindle dynamics.

ACKNOWLEDGEMENTS

We thank Elmar Schiebel for the Cdc14–GFP construct, Mensur Dlakic for Rrp14p alignment studies, Vincent Archambault for the *mec1Δ/sml1Δ* strain and Fred Cross for the *bub2Δ* strain. We thank Kevin Hardwick for the Spc42–GFP strain, the *mad2Δ* construct and for helpful comments on the manuscript. M.O. was the recipient of a post-doctoral fellowship by the Charles Revson Foundation. This work was supported by the Wellcome Trust. Funding to pay the Open Access publication charges for this article was provided by the Wellcome Trust.

Conflict of interest statement. None declared.

REFERENCES

- Warner,J.R. (1989) Synthesis of Ribosomes in *Saccharomyces cerevisiae*. *Microbiol. Rev.*, **53**, 256–271.
- Rudra,D. and Warner,J.R. (2004) What better measure than ribosome synthesis? *Genes Dev.*, **18**, 2431–2436.
- Ju,Q. and Warner,J.R. (1994) Ribosome synthesis during the growth cycle of *Saccharomyces cerevisiae*. *Yeast*, **10**, 151–157.
- Dez,C., Froment,C., Noaillic-Depeyre,J., Monsarrat,B., Caizergues-Ferrer,M. and Henry,Y. (2004) Npa1p, a component of very early Pre-60S ribosomal particles, associates with a subset of small nucleolar RNPs required for peptidyl transferase center modification. *Mol. Cell. Biol.*, **24**, 6324–6337.
- Du,Y.C. and Stillman,B. (2002) Yph1p, an ORC-interacting protein. potential links between cell proliferation control, DNA replication, and ribosome biogenesis. *Cell*, **109**, 835–848.
- Oeffinger,M. and Tollervey,D. (2003) Yeast Nop15p is an RNA-binding protein required for pre-rRNA processing and cytokinesis. *EMBO J.*, **22**, 6573–6583.
- Dosil,M. and Bustelo,X.R. (2004) Functional characterization of Pwp2, a WD family protein essential for the assembly of the 90 S pre-ribosomal particle. *J. Biol. Chem.*, **279**, 37385–37397.
- Saracino,F., Bassler,J., Muzzini,D., Hurt,E. and Agostoni Carbone,M.L. (2004) The yeast kinase Swe1 is required for proper entry into cell cycle after arrest due to ribosome biogenesis and protein synthesis defects. *Cell Cycle*, **3**, 648–654.
- Shafaatian,R., Payton,M.A. and Reid,J.D. (1996) PWP2, a member of the WD-repeat family of proteins, is an essential *Saccharomyces cerevisiae* gene involved in cell separation. *Mol. Gen. Genet.*, **252**, 101–114.
- Bogomolnaya,L.M., Pathak,R., Cham,R., Guo,J., Surovtseva,Y.V., Jaekel,L. and Polymenis,M. (2004) A new enrichment approach identifies genes that alter cell cycle progression in *Saccharomyces cerevisiae*. *Curr. Genet.*, **45**, 350–359.
- Drees,B.L., Sundin,B., Brazeau,E., Caviston,J.P., Chen,G.C., Guo,W., Kozminski,K.G., Lau,M.W., Moskow,J.J., Tong,A. *et al.* (2001) A protein interaction map for cell polarity development. *J. Cell Biol.*, **154**, 549–571.
- Roy,N. and Runge,K.W. (2000) Two paralogs involved in transcriptional silencing that antagonistically control yeast life span [In Process Citation]. *Curr. Biol.*, **10**, 111–114.
- Yu,Y. and Hirsch,J.P. (1995) An essential gene pair in *Saccharomyces cerevisiae* with a potential role in mating. *DNA Cell Biol.*, **14**, 411–418.
- Hofken,T. and Schiebel,E. (2004) Novel regulation of mitotic exit by the Cdc42 effectors Gic1 and Gic2. *J. Cell Biol.*, **164**, 219–231.
- Brown,J.L., Jaquenoud,M., Gulli,M.P., Chant,J. and Peter,M. (1997) Novel Cdc42-binding proteins Gic1 and Gic2 control cell polarity in yeast. *Genes Dev.*, **11**, 2972–2982.
- Chen,G.-C., Kim,Y.-J. and Chan,C.S.M. (1997) The Cdc42 GTPase-associated proteins Gic1 and Gic2 are required for polarized cell growth in *Saccharomyces cerevisiae*. *Genes Dev.*, **11**, 2958–2971.
- Fatica,A., Cronshaw,A.D., Dlakic,M. and Tollervey,D. (2002) Ssf1p prevents premature processing of an early pre-60S ribosomal particle. *Mol. Cell*, **9**, 341–351.
- Magoulas,C., Zatzepina,O.V., Jordan,P.W., Jordan,E.G. and Fried,M. (1998) The SURF-6 protein is a component of the nucleolar matrix and has a high binding capacity for nucleic acids *in vitro*. *Eur. J. Cell Biol.*, **75**, 174–183.
- Hazbun,T.R., Malmstrom,L., Anderson,S., Graczyk,B.J., Fox,B., Riffle,M., Sundin,B.A., Aranda,J.D., McDonald,W.H., Chiu,C.H. *et al.* (2003) Assigning function to yeast proteins by integration of technologies. *Mol. Cell*, **12**, 1353–1365.
- Polzikov,M., Zatzepina,O. and Magoulas,C. (2005) Identification of an evolutionary conserved SURF-6 domain in a family of nucleolar proteins extending from human to yeast. *Biochem. Biophys. Res. Commun.*, **327**, 143–149.
- Longtine,M.S., McKenzie,A., 3rd, Demarini,D.J., Shah,N.G., Wach,A., Brachat,A., Philippsen,P. and Pringle,J.R. (1998) Additional modules for versatile and economical PCR-based gene deletion and modification in *Saccharomyces cerevisiae*. *Yeast*, **14**, 953–961.
- Rigaut,G., Shevchenko,A., Rutz,B., Wilm,M., Mann,M. and Seraphin,B. (1999) A generic protein purification method for protein complex characterization and proteome exploration. *Nat. Biotechnol.*, **17**, 1030–1032.
- Kufel,J., Allmang,C., Chanfreau,G., Petfalski,E., Lafontaine,D.L.J. and Tollervey,D. (2000) Precursors to the U3 snoRNA lack snoRNP proteins but are stabilized by La binding. *Mol. Cell Biol.*, **20**, 5415–5124.
- Tollervey,D., Lehtonen,H., Jansen,R., Kern,H. and Hurt,E.C. (1993) Temperature-sensitive mutations demonstrate roles for yeast fibrillarlin in pre-rRNA processing, pre-rRNA methylation, and ribosome assembly. *Cell*, **72**, 443–457.
- Blabler,J., Grandi,P., Gadal,O., Lebmann,T., Petfalski,E., Tollervey,D., Lechner,J. and Hurt,E. (2001) Identification of a 60S pre-ribosomal particle that is closely linked to nuclear export. *Mol. Cell*, **8**, 517–529.

26. Fraser, R.S. and Moreno, F. (1976) Rates of synthesis of polyadenylated messenger RNA and ribosomal RNA during the cell cycle of *Schizosaccharomyces pombe*. With an appendix: calculation of the pattern of protein accumulation from observed changes in the rate of messenger RNA synthesis. *J. Cell Sci.*, **21**, 497–521.
27. Grandi, P., Doyl, V. and Hurt, E.C. (1993) Purification of NSP1 reveals complex formation with 'GLFG' nucleoporins and a novel nuclear pore protein NIC96. *EMBO J.*, **12**, 3061–3071.
28. Bergès, T., Petfalski, E., Tollervey, D. and Hurt, E.C. (1994) Synthetic lethality with fibrillarlin identifies NOP77p, a nucleolar protein required for pre-rRNA processing and modification. *EMBO J.*, **13**, 3136–3148.
29. Aris, J.P. and Blobel, G. (1991) cDNA cloning and sequencing of human fibrillarlin, a conserved nucleolar protein recognized by autoimmune antisera. *Proc. Natl Acad. Sci. USA*, **88**, 931–935.
30. Horsey, E.W., Jakovljevic, J., Miles, T.D., Harnpicharnchai, P. and Woolford, J.L., Jr (2004) Role of the yeast Rrp1 protein in the dynamics of pre-ribosome maturation. *RNA*, **10**, 813–827.
31. Krogan, N.J., Cagney, G., Yu, H., Zhong, G., Guo, X., Ignatchenko, A., Li, J., Pu, S., Datta, N., Tikuisis, A.P. *et al.* (2006) Global landscape of protein complexes in the yeast *Saccharomyces cerevisiae*. *Nature*, **440**, 637–643.
32. Fatica, A., Oeffinger, M., Tollervey, D. and Bozzoni, I. (2003) Cic1p/Nsa3p is required for synthesis and nuclear export of 60S ribosomal subunits. *RNA*, **9**, 1431–1436.
33. Rosado, I.V. and de la Cruz, J. (2004) Npa1p is an essential trans-acting factor required for an early step in the assembly of 60S ribosomal subunits in *Saccharomyces cerevisiae*. *RNA*, **10**, 1073–1083.
34. Jimenez, J., Cid, V.J., Cenamor, R., Yuste, M., Molero, G., Nombela, C. and Sanchez, M. (1998) Morphogenesis beyond cytokinetic arrest in *Saccharomyces cerevisiae*. *J. Cell Biol.*, **143**, 1617–1634.
35. Hofken, T. and Schiebel, E. (2002) A role for cell polarity proteins in mitotic exit. *EMBO J.*, **21**, 4851–4862.
36. Snyder, M., Gehrung, S. and Page, B.D. (1991) Studies concerning the temporal and genetic control of cell polarity in *Saccharomyces cerevisiae*. *J. Cell Biol.*, **114**, 515–532.
37. Jacobs, C.W., Adams, A.E., Szaniszló, P.J. and Pringle, J.R. (1988) Functions of microtubules in the *Saccharomyces cerevisiae* cell cycle. *J. Cell Biol.*, **107**, 1409–1426.
38. Straight, A.F., Shou, W., Dowd, G.J., Turck, C.W., Deshaies, R.J., Johnson, A.D. and Moazed, D. (1999) Net1, a Sir2-associated nucleolar protein required for rDNA silencing and nucleolar integrity. *Cell*, **97**, 245–256.
39. Shou, W., Seol, J.H., Shevchenko, A., Baskerville, C., Moazed, D., Chen, Z.W., Jang, J., Shevchenko, A., Charbonneau, H. and Deshaies, R.J. (1999) Exit from mitosis is triggered by Tem1-dependent release of the protein phosphatase Cdc14 from nucleolar RENT complex. *Cell*, **97**, 233–244.
40. Visintin, R., Hwang, E.S. and Amon, A. (1999) Cfl1p prevents premature exit from mitosis by anchoring Cdc14 phosphatase in the nucleolus. *Nature*, **398**, 818–823.
41. Yang, C.H., Lambie, E.J., Hardin, J., Craft, J. and Snyder, M. (1989) Higher order structure is present in the yeast nucleus: autoantibody probes demonstrate that nucleolus lies opposite the spindle pole body. *Chromosoma*, **98**, 123–128.
42. Musacchio, A. and Hardwick, K.G. (2002) The spindle checkpoint: structural insights into dynamic signalling. *Nature Rev. Mol. Cell Biol.*, **3**, 731–741.
43. Chen, R.H., Brady, D.M., Smith, D., Murray, A.W. and Hardwick, K.G. (1999) The spindle checkpoint of budding yeast depends on a tight complex between the Mad1 and Mad2 proteins. *Mol. Biol. Cell*, **10**, 2607–2618.
44. Daum, J.R., Gomez-Ospina, N., Winey, M. and Burke, D.J. (2000) The spindle checkpoint of *Saccharomyces cerevisiae* responds to separable microtubule-dependent events. *Curr. Biol.*, **10**, 1375–1378.
45. Zhang, Y., Yu, Z., Fu, X. and Liang, C. (2002) Noc3p, a BHLH protein, plays an integral role in the initiation of DNA replication in budding yeast. *Cell*, **109**, 849–860.
46. Bernstein, K.A. and Baserga, S.J. (2004) The small subunit processome is required for cell cycle progression at G1. *Mol. Biol. Cell*, **15**, 5038–5046.
47. Weinert, T.A., Kiser, G.L. and Hartwell, L.H. (1994) Mitotic checkpoint genes in budding yeast and the dependence of mitosis on DNA replication and repair. *Genes Dev.*, **8**, 652–665.
48. Jorgensen, P., Nishikawa, J.L., Breitenkreutz, B.J. and Tyers, M. (2002) Systematic identification of pathways that couple cell growth and division in yeast. *Science*, **297**, 395–400.
49. Jorgensen, P., Tyers, M. and Warner, J.R. (2003) In Hall, M.N., Raff, M. and Thomas, G. (eds), *Cell Growth: Control of Cell Size*. Cold Spring Harbor Laboratory Press, Cold Spring Harbor, pp. 329–370.
50. Bystricky, K., Laroche, T., van Houwe, G., Blaszczyk, M. and Gasser, S.M. (2005) Chromosome looping in yeast: telomere pairing and coordinated movement reflect anchoring efficiency and territorial organization. *J. Cell Biol.*, **168**, 375–387.
51. Kinoshita, Y., Jarell, A.D., Flaman, J.M., Foltz, G., Schuster, J., Sopher, B.L., Irvin, D.K., Kanning, K., Kornblum, H.I., Nelson, P.S. *et al.* (2001) Pescadillo, a novel cell cycle regulatory protein abnormally expressed in malignant cells. *J. Biol. Chem.*, **276**, 6656–6665.
52. Li, R. and Murray, A.W. (1991) Feedback control of mitosis in budding yeast. *Cell*, **66**, 519–531.
53. Luo, X., Tang, Z., Rizo, J. and Yu, H. (2002) The Mad2 spindle checkpoint protein undergoes similar major conformational changes upon binding to either Mad1 or Cdc20. *Mol. Cell*, **9**, 59–71.
54. Alliegro, M.C., Alliegro, M.A. and Palazzo, R.E. (2006) Centrosome-associated RNA in surf clam oocytes. *Proc. Natl Acad. Sci. USA*, **103**, 9034–9038.
55. Blower, M.D., Nachury, M., Heald, R. and Weis, K. (2005) A Rae1-containing ribonucleoprotein complex is required for mitotic spindle assembly. *Cell*, **121**, 223–234.
56. Larsen, N.A. and Harrison, S.C. (2004) Crystal structure of the spindle assembly checkpoint protein Bub3. *J. Mol. Biol.*, **344**, 885–892.
57. Murphy, R., Watkins, J.L. and Wente, S.R. (1996) GLE2, a *Saccharomyces cerevisiae* homologue of the *Schizosaccharomyces pombe* export factor RAE1, is required for nuclear pore complex structure and function. *Mol. Biol. Cell*, **7**, 1921–1937.
58. Moy, T.I. and Silver, P.A. (1999) Nuclear export of the small ribosomal subunit requires the ran-GTPase cycle and certain nucleoporins. *Genes Dev.*, **13**, 2118–2133.
59. Stage-Zimmermann, T., Schmidt, U. and Silver, P.A. (2000) Factors affecting nuclear export of the 60S ribosomal subunit *in vivo*. *Mol. Biol. Cell*, **11**, 3777–3789.
60. Fujiyama, S., Yanagida, M., Hayano, T., Miura, Y., Isobe, T. and Takahashi, N. (2002) Isolation and proteomic characterization of human parvulin-associating preribosomal ribonucleoprotein complexes. *J. Biol. Chem.*, **277**, 23773–23780.